A Bioengineering Approach to Myopia Control Tested in a Guinea Pig Model

Mariana B. Garcia,[1] Amit K. Jha,[2,3] Kevin E. Healy,[2,3] and Christine F. Wildsoet[1–3]

[1]Vision Science Graduate Group, University of California-Berkeley, Berkeley, California, United States
[2]Department of Bioengineering, University of California-Berkeley, Berkeley, California, United States
[3]Department of Materials Science and Engineering, University of California-Berkeley, Berkeley, California, United States

Correspondence: Mariana B. Garcia, 149 Commonwealth Drive, Menlo Park, CA 94025, USA; mariana.b.garcia@gmail.com.

Submitted: September 5, 2016
Accepted: February 21, 2017

Citation: Garcia MB, Jha AK, Healy KE, Wildsoet CF. A bioengineering approach to myopia control tested in a guinea pig model. *Invest Ophthalmol Vis Sci*. 2017;58:1875–1886. DOI: 10.1167/iovs.16-20694

Purpose. To investigate the biocompatibility of an injectable hydrogel and its ability to control myopia progression in guinea pigs.

Methods. The study used a hydrogel synthesized from acrylated hyaluronic acid with a conjugated cell-binding peptide and enzymatically degradable crosslinker. Seven-day-old guinea pigs were first form deprived (FD) with diffusers for 1 week. One group was kept as an FD-only control; two groups received a sub-Tenon's capsule injection of either hydrogel or buffer (sham surgery) at the posterior pole of the eye. Form deprivation treatments were then continued for 3 additional weeks. Treatment effects were evaluated in terms of ocular axial length and refractive error. Safety was evaluated via intraocular pressure (IOP), visual acuity, flash electroretinograms (ERG), and histology.

Results. Both hydrogel and sham surgery groups showed significantly reduced axial elongation and myopia progression compared to the FD-only group. For axial lengths, net changes in interocular difference (treated minus control) were 0.04 ± 0.06, 0.02 ± 0.09, and 0.24 ± 0.08 mm for hydrogel, sham, and FD-only groups, respectively ($P = 0.0006$). Intraocular pressures, visual acuities, and ERGs of treated eyes were not significantly different from contralateral controls. Extensive cell migration into the implants was evident. Both surgery groups showed noticeable Tenon's capsule thickening.

Conclusions. Sub-Tenon's capsule injections of both hydrogel and buffer inhibited myopia progression, with no adverse effects on ocular health. The latter unexpected effect warrants further investigation as a potential novel myopia control therapy. That the hydrogel implant supported significant cell infiltration offers further proof of its biocompatibility, with potential application as a tool for drug and cell delivery.

Keywords: myopia, sclera, guinea pig

Myopia (nearsightedness) is an ocular condition characterized by a mismatch between the eye's length and its refractive power, with the former being too long in relative or absolute terms. The net optical consequence is that images of distant objects fall in front of the retina for the uncorrected eye.[1] Myopia is estimated to affect 22% of the world's population (1.5 billion people)[2] and its prevalence continues to rise, precipitously so in East Asia,[3,4] with significant increases also reported in the United States,[5] Canada,[6] and Europe.[7] Apart from these changing prevalence statistics, of additional concern is the fact that the age of myopia onset has significantly decreased.[8] Since myopia tends to progress through adolescence, early onset allows more time for myopia to progress, with likely higher myopia endpoints and associated increased risk of complicating ocular pathology.[9]

Fundamental to the increase in eye size that typically underlies myopia is increased extracellular matrix (ECM) remodeling in the sclera, which comprises the outer fibrous supportive shell of the posterior vitreous chamber of the human eye. The changes in ECM reflect increased production of matrix metalloproteases (MMPs)[10] coupled to decreased production of tissue inhibitors of matrix metalloproteases (TIMPs), and are accompanied by decreases in ECM synthesis and proliferation of scleral fibroblasts.[11–15] The net result is a marked decrease in the total scleral ECM content, which in turn leads to thinning and mechanical weakening of the sclera.[16] The resulting increased creep (higher elongation under constant load), which characterizes the myopic sclera,[17–20] is especially pronounced at the posterior pole of highly myopic eyes and can lead to localized ecstasia (staphylomas). As alluded to above, the risks of vision-threatening conditions such as maculopathies, lacquer cracks, chorioretinal atrophy, and retinal detachment[21] all increase with the amount of myopia.[9] These pathologies reflect changes in the tissues adjacent to the sclera—retina, retinal pigment epithelium, and choroid, all of which are subject to stretching forces as the sclera shell expands.[22,23]

Current treatments for controlling myopia progression are largely limited to optical and pharmacologic strategies, with few targeting the sclera directly. In the latter category, scleral reinforcement (buckling) surgery targets highly myopic eyes with mechanically unstable scleras. Collagen crosslinking treatments, adapted from corneal therapies (e.g., for keratoconus), have also been tested in animal models to increase scleral rigidity and slow myopia progression.[24] Chemical crosslinking strategies using glyceraldehyde[25] and genipin[26–28] avoid the

risk of toxic damage to the retina presented by UV photoinitiation options such as those involving riboflavin.[29] Crosslinking strategies also present delivery challenges, including the need for multiple parabulbar injections to achieve adequate scleral coverage[25,26,27] and limiting crosslinking in adjacent tissues, including the walls of major blood vessels. Finally, the potential long-term negative implications of excessive increases in scleral rigidity and how they might impact the health of the retina and choroid remain unknown.

In the study reported here we tested an injectable hydrogel, implanted against the sclera, as an approach for slowing myopia progression. The conceptual framework for this approach is that the implantation of a cell-responsive hydrogel against the sclera could serve as a scaffold into which scleral fibroblasts migrate and lay down new matrix, thereby increasing scleral thickness and potentially decreasing associated creep. By opposing or reversing the changes characteristic of myopic scleras, excessive eye elongation could be slowed or halted, the level of myopia contained, and so, the risk of associated vision-threatening conditions reduced.

Hydrogel-based cell-free therapies to support native tissue stability have been proposed for corneal applications[30–33] and some have shown promising results in clinical trials.[31] Note that an earlier (mid-1990s) clinical study involving sub-Tenon's capsule injection of a gel foam in humans reported slowed myopia progression, but only limited study details are available and there have been no follow-up reports.[34–36] Both the latter approach and our proposed approach are less invasive than the current scleral buckling surgery used to treat high myopia[37,38] and do not rely on availability of donor tissue.

The current study made use of the guinea pig as a mammalian model for myopia and a hyaluronic acid–based hydrogel.[39] This work is a follow-up to our earlier studies testing two different hydrogels—one based on polyvinypyrrolidone[35] and another based on N-isopropylacrylamide[36]—in the chick, which has been widely used as an animal model for myopia. However, for sclera-directed therapies, the chick's bilayered sclera limits the translational potential of results to humans.[34–36]

Over the last few years, guinea pigs have emerged as an important myopia animal model. For the current study, they combine the advantage of mammalian eyes—sclera composed only of fibrous collagen with no underlying cartilage layer, unlike the avian sclera—with substantially larger eyes than other rodents, along with ease of housing and husbandry compared to nonhuman primates. With their increasing popularity as a myopia model, their emmetropization process has now been well characterized,[40,41] as have their responses to both form deprivation[42] and imposed defocus.[43]

Various properties were taken into account when considering potential options for an injectable hydrogel, including biocompatibility with scleral fibroblasts and ability to allow for independent modulation of mechanical, cell-binding, and degradation properties. A hyaluronic acid–based hydrogel was ultimately selected for testing in our mammalian model.[39,44–46] Hyaluronic acid (HyA) was a logical choice as it is widely distributed throughout the eye, as is the enzyme hyaluronidase, which is responsible for its degradation.[47] In brief, the chosen hydrogel consists of two distinct macromers: acrylated hyaluronic acid (AcHyA) and a cell-binding peptide, bsp-RGD(15), conjugated to yield acrylated hyaluronic acid (AcHyA-RGD). The RGD-containing peptide was selected because of its known affinity for the integrin subunits identified in the mammalian sclera.[48–51] The inclusion of a MMP-degradable peptide as a crosslinker allowed for cell-mediated control over the rate of degradation of the hydrogel, with the specific choice allowing for degradation by MMP-9, MMP-2, and MMP-13,[52] which have been detected in mammalian sclera.[47,53,54]

Materials and Methods

Animals

Pigmented English short-hair guinea pig pups were weaned at 5 days of age and raised in transparent plastic wire-top cages, under a 12-hour/12-hour light/dark cycle, with free access to water and vitamin C–supplemented food. They also received fresh fruit and vegetables three times a week as diet enrichment. All animal care and treatments in this study conformed to the ARVO Statement for the Use of Animals in Ophthalmic and Vision Research, and all experimental protocols were approved by the Animal Care and Use Committee of the University of California-Berkeley.

Hydrogel Synthesis

A soft, 2% wt/vol HyA hydrogel was selected for this application based on results from a pilot in vivo experiment using a stiffer (3% wt/vol, 800 Pa) formulation, which resulted in significant scleral indentation and globe distortion after injection. Details of the in vitro studies underpinning the final design, including rheologic characterization of synthesized hydrogels, are described elsewhere.[55] The shear modulus of the selected HyA hydrogel was ~200 Pa.[39,55]

The protocol for synthesizing the HyA-based hydrogel has been previously reported and is described in brief here.[55,44] An HyA derivative carrying hydrazide groups (HyAADH) was first synthesized by reacting adipic acid dihydrazide in the presence of EDC (ethyl-(3-dimethylaminopropyl)carbodiimide hydrochloride) and HOBt (1-Hydroxybenzotriazole hydrate) at pH 6.8.[56,57] Acrylate (Ac) groups were subsequently conjugated to the hydrazide groups on HyAADH through reaction with acryloxysuccinimide, thereby generating AcHyA.[39] The success of this conjugation procedure was confirmed by ^{1}H NMR. The AcHyA-RGD derivative was synthesized by reacting the peptide bsp-RGD(15) (CGGNGEPRGDTYRAY) with AcHyA at room temperature.

The latter two macromers were used to synthesize the final product (2% wt/vol hydrogel with 380 μM RGD) by first dissolving them in triethanolamine buffer (TEA; 0.3 M, pH 8), incubating the solution for 15 minutes at 37°C, and finally reacting the solution with the MMP-cleavable peptide, CQPQGLAKC,[39,52,58] added to create a 1:1 molar ratio between the Ac groups in the HyA macromer and the cysteine groups in the crosslinker. The last two steps were performed immediately before surgical implantation to allow for polymerization in situ.

Experimental Design and Procedures

Experimental Design. A schematic of the experimental design is provided in Figure 1. In brief, young guinea pigs were monocularly form deprived to induce myopia. One control group of animals underwent form deprivation only. All other animals underwent implantation surgery on their form-deprived eyes, involving either the HyA hydrogel or TEA buffer (sham). To characterize the treatment effects, a variety of biometric and functional data were collected over the experimental period, after which the animals were euthanized and ocular tissue was processed for histology. Measurements were limited to daytime hours to avoid any confounding effect of exposing the animals to light during their nocturnal cycles.

Visual Manipulation and Implants. To induce form-deprivation (FD) myopia, guinea pigs were fitted with white

Investigative Ophthalmology & Visual Science

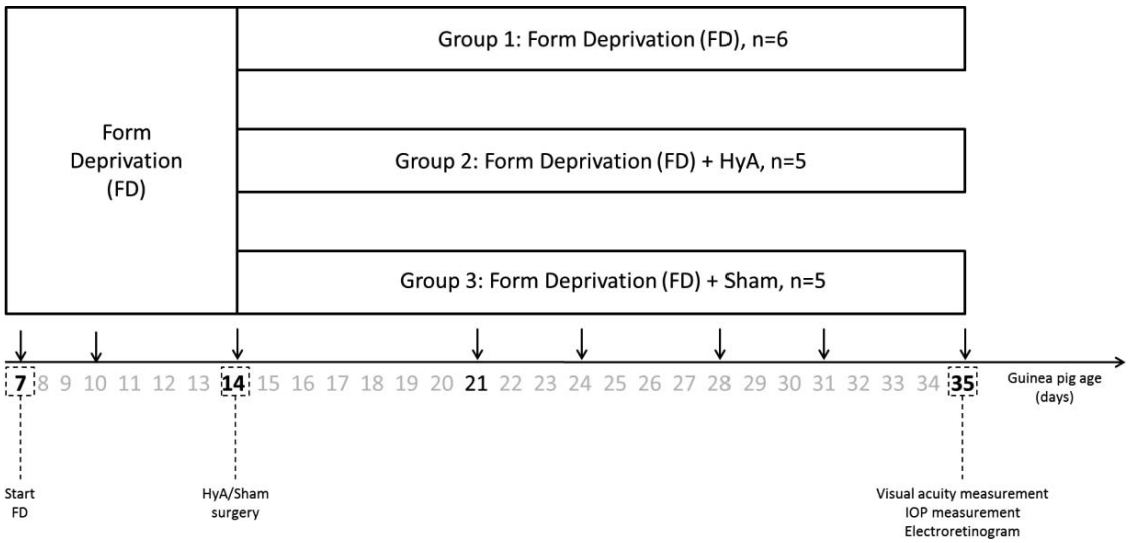

Figure 1. Schematic representation of experimental design and measurement schedule. Seven-day-old guinea pigs were fitted with monocular diffusers to induce form deprivation (FD) myopia and assigned to one of three treatment groups: form deprivation (FD)-only, FD + HyA sub-Tenon's capsule injection, and FD + Sham (TEA buffer) sub-Tenon's capsule injection. Ocular axial lengths were measured using high-resolution A-scan ultrasonography eight times, at ages indicated by the *arrows*, and cycloplegic refractions were undertaken at ages 7, 21, and 35 days.

plastic diffusers. Only animals in which the diffuser-treated eye had grown by 50 μm more than its contralateral control after 7 days of treatment were included in the study, to improve our ability to detect the myopia control effects of planned surgical interventions. Animals were then randomly assigned into one of three groups: FD-only group, FD + HyA group, or FD + Sham group ($n = 5$–6 per group). On experimental day 7 (14 days of age), the FD + HyA group received a sub-Tenon's capsule injection of 80 μL HyA hydrogel while the FD + Sham group received a sub-Tenon's capsule injection of 80 μL of the buffer used to dissolve the HyA macromers (0.2 M triethanolamine buffer, TEA; Sigma-Aldrich Corp., St. Louis, MO, USA). The diffusers were replaced immediately after the implantation surgery. All three groups wore their diffusers for a further 21 days (until 35 days of age).

The dome-shaped diffusers employed in this study were prepared by hot molding white styrene (Midwest Products Co., Hobart, IN, USA). Diffusers were then mounted on hook Velcro ring supports (Velcro Industries, Manchester, NH, USA) with UV-curing glue (Norland Products, Cranbury, NJ, USA). Only diffusers with transmittance of 15% ± 1% were used in this study. To attach the diffusers to the guinea pigs, four 1/8 sections of rings of loop Velcro were affixed symmetrically to the fur surrounding the eye using gel cyanoacrylate glue (SureHold Plastic Surgery, Chicago, IL, USA).[42]

Sub-Tenon's Capsule Implantation Surgery. Animals received a sub-Tenon's capsule injection at the posterior pole, consisting of 80 μL of either the custom-designed HyA hydrogel or 0.2 M TEA buffer under sterile conditions with the aid of a surgical microscope. Guinea pigs were first anesthetized with a ketamine/xylazine cocktail (45/4.5 mg/kg body weight). A drop of topical local anesthetic (0.5% proparacaine hydrochloride; Bausch & Lomb, Rochester, NY, USA) was applied to the cornea, and an eyelid retractor was inserted to increase visibility of the superior aspect of the eye during surgery. To facilitate access to the posterior sclera, an anchor suture (Reli Plain Gut 5-0; Myco Medical Supplies, Apex, NC, USA) was inserted through the superior bulbar conjunctiva and used to rotate the eye in a nasal direction, after which an incision (5–10 mm wide) was made through the conjunctiva, episclera, and Tenon's capsule to expose the sclera. The sclera was further separated from overlying tissues at the posterior pole of the eye using blunt forceps, thus creating a space to receive the injected HyA or buffer. The incision was loosely closed using a loop suture (6-0 or 7-0 silk suture; Ethicon, Somerville, NJ, USA). Injections were slowly delivered from a zero-dead-volume syringe fitted with a curved 19G retrobulbar injection needle (Beaver-Visitec, Waltham, MA, USA), which was threaded through the loop suture to reach the posterior pole. The loop suture was progressively closed as the needle was withdrawn to minimize leakage of solution from the injection site, then finally fully closed and tied off. Note that the HyA solution was prepared (by mixing HyA precursors with crosslinker) immediately before its injection to avoid polymerization in the needle. Topical moxifloxacin hydrochloride solution (Vigamox; Alcon, Ft. Worth, TX, USA) was applied prophylactically to the incision site, the lid retractor removed, and any blood or fluid gently cleared away with sterile gauze. Diffusers were replaced and the guinea pigs were allowed to recover from anesthesia. Topical moxiflocaxin was instilled once daily for 2 days following the surgery. Over the remainder of the study period, the operated eyes were closely monitored for signs of inflammation (redness, swelling, discharge, eyelid ptosis).

Measurement of Refractive Error and Ocular Dimensions. Refractive errors were measured using streak retinoscopy on awake animals, 30 minutes after instillation of 1% cyclopentolate hydrochloride (Bausch & Lomb), on experimental days 0, 14, and 28. Noncycloplegic refractions were also undertaken on day 7, prior to surgery. Refractive errors are reported as spherical equivalent refractions (SERs; average of the results for the two principal meridians).

To obtain ocular axial length data, high resolution A-scan ultrasonography measurements (~10 μm resolution)[59,60] were made under gaseous anesthesia (2.5–3% isoflurane in oxygen) on experimental day 0 (age 7 days) and approximately twice a week thereafter, excepting experimental day 10 (3 days after surgery). The last measurement was performed on experimental day 28. Measurements on individual animals were conducted at the same time of day to avoid possible confounding effects of circadian rhythms in eye growth.[61] Referred to hereafter as axial length, it represents the sum of anterior chamber, lens, and vitreous chamber axial dimensions. At least seven recordings were averaged per time point to obtain

reported data. The boundaries of the HyA implants could not be distinguished in captured traces.

Magnetic Resonance Imaging (MRI). To qualitatively assess the regional distribution of the polymer after implantation surgery, one 2-week-old guinea pig underwent magnetic resonance imaging 2 days after undergoing the surgery as described above. Imaging made use of an 7T 300 MHz Horizontal Bore MRI System (Varian, Palo Alto, CA, USA), with a 20 G/cm 205-mm high-duty cycle gradient coil, and an SA Instruments Animal Monitoring System (Stony Brook, NY, USA), complete with heating and respiratory monitoring accessories. The imaging protocol made use of a surface coil positioned over the eye to be imaged. The guinea pig was anesthetized with 3% isoflurane in oxygen for this procedure, with artificial tear gel applied to the corneas of both eyes to prevent them from drying during imaging. No contrast agents were used. T2-weighted images were acquired using a spin-echo multislice imaging sequence. The resolution of the system was 100 μm, slice size was 0.8 mm, and field of view was 2.6 cm.

Functional Tests. To rule out adverse effects of the surgery, including toxic effects of the implanted hydrogels, retinal activity and visual acuity were assessed on the last day of the monitoring period. Flash electroretinography (ERG) was recorded with an Espion small animal unit (Diagnosys, Lowell, MA, USA) and visual acuity was recorded with an OptoMotry device (CerebralMechanics, Lethbride, Alberta, Canada). For flash ERG recordings, guinea pigs were first anesthetized with a subcutaneous injection of ketamine/xylazine (45/4.5 mg/kg body weight, respectively). Pupils were dilated with two drops of 1% cyclopentolate and lid retractors were inserted to hold both eyes open. DTL electrodes (Diagnosys) were placed over the lower cornea of each eye, close to the lower lid margin. Hydroxypropyl methylcellulose gel (2.5%, EyeGel; Eyesupply USA, Tampa, FL, USA) was instilled to stabilize the electrodes and to prevent the corneas from drying during the recording session. Reference and ground electrodes (subcutaneous platinum needles, Diagnosys) were placed in the mouth (over the tongue and behind the incisor teeth) and under the neck skin, respectively. Flash ERG stimuli were delivered simultaneously via two Ganzfeld stimulators (50-mm internal diameter, Diagnosys ColorBurst) centered in front of each eye. After 10 minutes of light adaptation at 3 cd/m^2, responses were recorded to stimuli comprising twenty 4-ms, 3 cd/m^2-white light flashes, separated by 1-second dark intervals. As indices of retinal function, amplitudes and implicit times (i.e., time from baseline to wave peak) were extracted for the a-wave, b-wave, and photopic negative response (PhNR) components, which reflect activities of the photoreceptors, inner nuclear layer, and ganglion cell layer, respectively.

Visual acuities were recorded using an OptoMotry device, which uses involuntary eye and/or head and body movements elicited in response to moving/revolving stimuli (i.e., the optokinetic reflex) as evidence of resolution. Guinea pigs were positioned at the center of its virtual cylinder and presented with drifting sine wave grating stimuli set to 100% contrast. Starting with a 12°/s grating, testing made use of built-in software driving a staircase testing protocol, with spatial frequency decreased step-wise until optokinetic responses were elicited. Each spatial frequency was tested five times.

For intraocular pressure (IOP) measurements, IOPs were measured in awake animals using a small animal rebound tonometer (Tonolab; iCare, Raleigh, NC, USA). All measurements were performed at the same time of day, in a quiet room with lights on, to avoid potentially confounding effect of stress and ocular circadian rhythms.

Histology. At the end of the 28-day treatments, guinea pigs were euthanized with an intracardiac injection of sodium pentobarbital (Euthasol; Virbac Animal Health, Ft. Worth, TX, USA) delivered under anesthesia (5% isoflurane in oxygen). Eyes were carefully enucleated and cleaned of excess extraorbital fat and muscle (taking care not to disturb any remnants of hydrogel implant), fixed overnight in 4% paraformaldehyde, and stored in 70% ethanol until further processed. For paraffin embedding, eyes were placed in a cassette, dehydrated using the protocol for a Shandon Excelsior (Thermo Fisher Scientific, Waltham, MA, USA) tissue automated processor, sliced in half using a microtome blade, and embedded using a paraffin mold with the cut surface facing down. Sections 5 μm thick were cut and stained with either a combination of hematoxylin and eosin, to visualize overall morphology, or hematoxylin and alcian blue, to highlight the HyA hydrogel. For both staining protocols, sections were rehydrated by serial incubations in xylene followed by decreasing concentrations of ethanol, from 100% to 0%. Sections were incubated for either 3 to 5 minutes in hematoxylin followed by 30 seconds in eosin, or 10 minutes in hematoxylin followed by 30 to 45 minutes in 1% alcian blue in 3% acetic acid. After staining, sections were dehydrated with increasing concentrations of ethanol followed by washes in xylene, then mounted in DPX mounting medium (Honeywell Fluka, Mexico City, Mexico) and imaged with an Axioplan 2 microscope (Carl Zeiss, Oberkochen, Germany).

Statistical Analysis and Data Representation

Statistical analyses were performed with GraphPad Prism 6 (La Jolla, CA, USA). For all three treatment groups, the differences between treated and contralateral (fellow) eyes were determined for all measured parameters and subsequently analyzed using a Wilcoxon matched pairs test. To compare the responses between treatment groups, interocular differences (treated eye minus control eye), or changes in interocular differences over the 28-day treatment normalized to baseline values (treated eye minus control eye at treatment day 28) minus (treated eye minus control eye at treatment day 0), were compared using a Mann-Whitney U test or Kruskal-Wallis test with Dunn's multiple comparisons post hoc test, as appropriate. P values lower than 0.05 were considered statistically significant. Data are graphically represented as box and whisker plots, showing median, minimum, and maximum values as well as 25th to 75th percentiles. Whenever numerical values are given in the text, they represent means ± standard deviations (SDs).

Results

The FD treatment applied to the young guinea pigs triggered an increase in ocular elongation and myopic changes in refractive error, as evident after 1 week of treatment. As was the goal of the HyA hydrogel intervention, FD eyes that were subjected to the surgery showed slowed elongation despite continued FD. Unexpectedly, FD eyes subjected to the sham surgery also showed slowed elongation. There was no evidence of adverse effects of these surgical interventions. The results of our study are described in more detail below.

MRI Localization of Implants

Acquisition parameters highlighted water-rich structures, making it an ideal tool to validate our implantation technique. Figure 2 shows an axial view of a guinea pig eye, imaged after receiving a sub-Tenon's capsule injection of HyA hydrogel. The hydrogel implant can clearly be seen encasing the posterior pole of the eye, as was the goal of the surgery. Note also that even though the needle used to inject the hydrogel was slowly

Investigative Ophthalmology & Visual Science

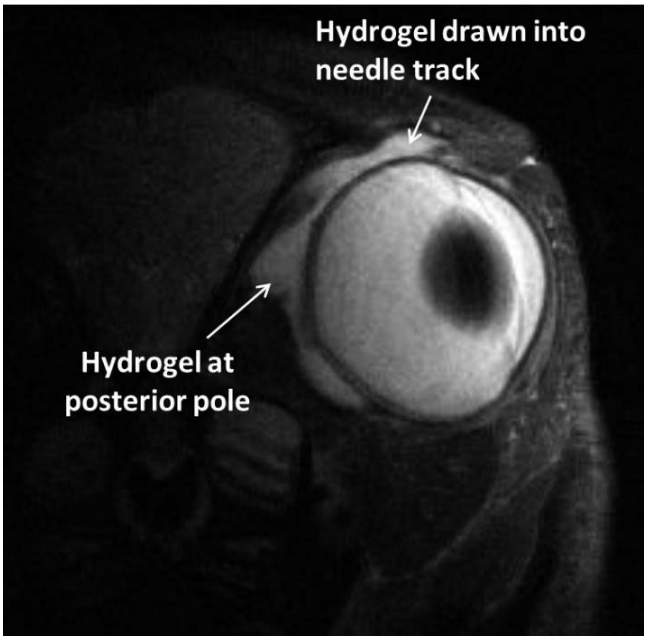

FIGURE 2. Image of an eye and surrounding orbital structures, acquired with a 7T MRI 2 days after injection of HyA hydrogel under Tenon's capsule at the posterior pole. The hydrogel can clearly be seen surrounding the posterior pole, with some "escape" over the superior ocular surface into the needle track.

withdrawn from the surgical site, it was inevitable that some hydrogel would be carried into the needle track, as evidenced by its "escape" into the superior orbit.

Treatment-Induced Biometric and Refractive Error Changes

Results are reported as changes in parameters for treated and contralateral control eyes, and as changes in interocular differences (CIDs, treated minus control) over the total monitoring period. Vitreous chamber depth and overall axial length data are summarized in the Table. Changes in axial length and vitreous chamber depth are also illustrated and described in more detail below. Additional data covering other ocular components (anterior chamber depth, lens thickness, retina, choroid, and sclera) are summarized in Supplementary Table S1 in the Supplemental Information section.

The FD treatment induced axial elongation in all eyes over the first 7 days. The CIDs for axial length, normalized to baseline values, are plotted as a function of time for all three groups in Figure 3. For the FD-only group, most of the axial length elongation in the diffuser-wearing eyes occurred over the first 7 days (0.17 mm out of the total 0.24-mm interocular elongation), although treated eyes remained significantly longer than their fellows over the entire treatment period. In contrast, the CIDs for the FD + HyA group decreased after the implantation surgery. Unexpectedly, a similar pattern was observed in the FD + Sham group, which also exhibited decreased axial elongation despite having received an injection of buffer only. For the FD + HyA and FD + Sham groups, CIDs remained somewhat constant over the remainder of the monitoring period.

Net changes over the 28-day study for axial length for the FD-only, FD + HyA, and FD + Sham groups are shown in Figure 4. Figure 4A depicts the CIDs, while Figure 4B shows changes in axial length plotted separately for treated and control eyes. For the FD-only group, diffuser-treated eyes elongated significantly more than their contralateral controls (0.75 ± 0.09 vs. 0.51 ± 0.11 mm, $P = 0.03$, Wilcoxon test), with a corresponding mean CID of 0.24 ± 0.08 mm. In contrast, the diffuser-treated eyes of the FD + HyA and FD + Sham groups did not elongate significantly more than their contralateral controls (0.61 ± 0.06 vs. 0.57 ± 0.09 mm for the FD + HyA group; 0.65 ± 0.07 vs. 0.63 ± 0.03 mm for the FD + Sham group). The CIDs for axial lengths of the FD group were also significantly larger than the CIDs for both FD + HyA and FD + Sham groups ($P = 0.0006$, Kruskal-Wallis test).

The axial length increases in myopia typically reflect increased elongation of the vitreous chambers. Consistent with the observations for axial lengths, the mean CID for vitreous chamber depth for the FD-only group is much larger than that for both FD + HyA and FD + Sham groups (Fig. 5A; 0.17 ± 0.14 vs. 0.01 ± 0.1 vs. –0.03 ± 0.09 mm, respectively). CIDs for vitreous chamber depths were significant for the FD-only as well as FD + Sham groups, although opposite in sign. There was also a strong and statistically significant correlation between CIDs for vitreous chamber depth and axial length for pooled data from individual animals ($r^2 = 0.80$, $P < 0.001$, Fig. 5B). There were no statistically significant differences in the anterior chamber depth and lens thickness CIDs (Kruskal-Wallis test).

Given the apparent inhibitor effects on ocular elongation of both surgical manipulations, and that with our hydrogel injections we had hoped to trigger cellular events (cell migration and matrix deposition) to thicken the sclera, it is of interest to examine scleral thickness (ST) changes. However, no significant CID of ST was observed for any of the treatment groups, the changes being negligible in all cases (0.00 ± 0.01 mm for FD group, –0.02 ± 0.03 for FD + HyA group, and 0.00 ± 0.03 mm for FD + Sham group; see also Supplementary Table S1; Supplementary Fig. S1). It is also not clear whether the ultrasonography technique used in this study would have detected recently added tissue due to likely differences in impedance.[36]

Figure 6 shows the net CIDs for refractive errors over the 28-day study period. These data are generally consistent with the trends observed for axial length, albeit more complex. By the end of the study period, there were significant differences between treated and control eyes for the FD-only group, but

TABLE. Changes in Axial Ocular Dimensions Over the 28-Day Treatment Period

Ocular Component	Group	Change in Untreated Eye, mm, Mean ± SD	Change in Control Eye, mm, Mean ± SD	*P* Value, Wilcoxon Test
Vitreous chamber depth	FD-only	0.205 ± 0.082	0.035 ± 0.140	0.0625
	FD + Sham	0.104 ± 0.093	0.122 ± 0.034	0.875
	FD + HyA	0.087 ± 0.046	0.098 ± 0.063	>0.999
Axial length: anterior chamber + lens + vitreous chamber	FD-only	0.754 ± 0.092	0.512 ± 0.115	0.031
	FD + Sham	0.624 ± 0.021	0.624 ± 0.06	>0.999
	FD + HyA	0.606 ± 0.063	0.634 ± 0.028	0.750

Investigative Ophthalmology & Visual Science

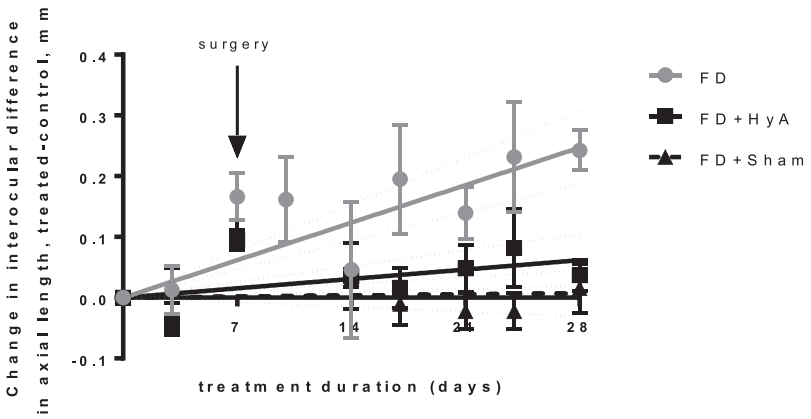

Figure 3. Changes from baseline in interocular axial length differences (CIDs, mean ± SEM) for FD-only, FD + HyA, and FD + Sham groups, plotted as a function of time. The *arrow* indicates timing of surgery (14 days of age). *Lines* derived from linear regression curve and 95% confidence interval bands (*dotted lines*) are superimposed onto the data points.

not for the other two groups ($P < 0.05$, Wilcoxon test). Nonetheless, nearly all treated eyes in the three treatment groups exhibited relative myopia (negative CIDs): five out of six animals in the FD-only group, five out of five in the FD + HyA group, and four out of five in the FD + Sham group. In none of the treatment groups did intergroup differences in CIDs reach statistical significance. It is noteworthy that the treated eyes of the FD + HyA group recorded the most relative myopia on the day of the surgery (day 7), though cycloplegia was not used to obtain these data and thus they are less reliable. Only the FD-only group showed continued myopia progression beyond treatment day 14. These two points are well illustrated in Figure 7, which shows the pattern of CID in refractive error over the study period for all three groups.

Acute Local Ocular Effects of the Surgeries

Immediately after surgery, no adverse effects were noted aside from slight transient redness around the incision site. In the days following the surgeries, no swelling, inflammation, or infection was observed in the surgical site in any of the FD + HyA and FD + Sham animals.

Effects of the Surgeries on Ocular Function and IOP

Electroretinographic data represent one of two sets of functional data collected to evaluate the safety of the surgical procedures and of the implanted hydrogel. Six parameters (amplitudes and implicit times for a-, and b-waves, and PhNR) were extracted from ERG recordings from FD + HyA and FD + Sham groups. Results for treated and contralateral eyes of both groups are summarized in Supplementary Table S2. For all six parameters, neither interocular differences for the two groups nor intergroup differences were found to be significant.

Visual acuities and IOPs were recorded as additional tests of the safety of the surgery and implanted hydrogel. For visual acuity, there was no significant difference between treated and

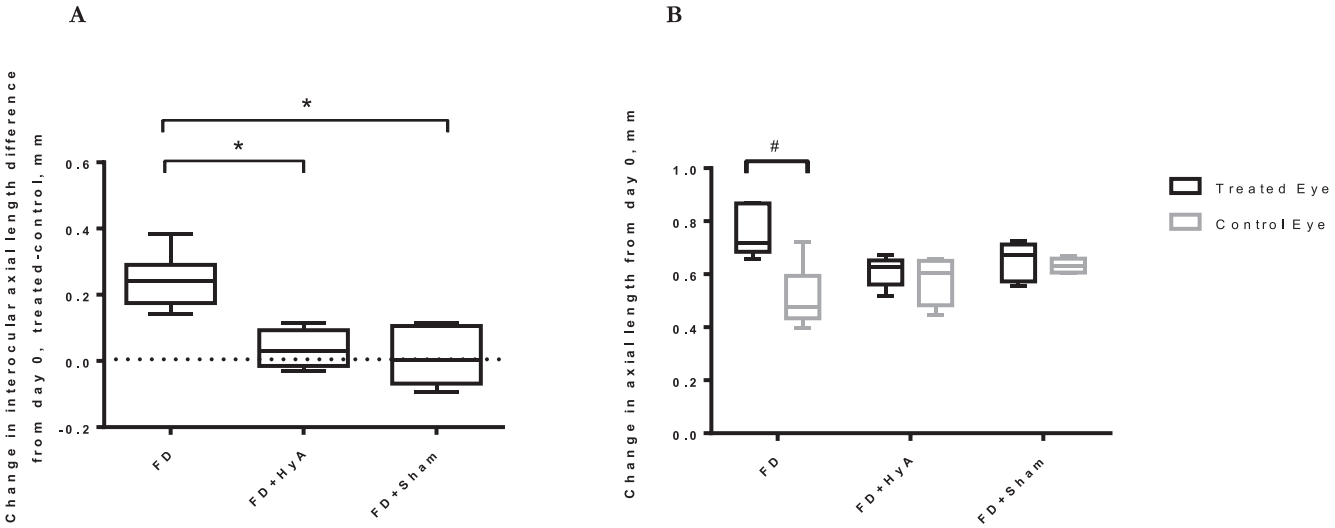

Figure 4. Box and whisker plots of (**A**) change in interocular difference in axial length and (**B**) change in axial length for treated and control eyes of FD-only, FD + HyA, and FD + Sham groups over the 28-day study period. *Box* encompasses upper and lower data quartiles; *whiskers* illustrate the upper and lower extremes of the data. (**A**) Changes in interocular differences (treated minus control); positive values indicate greater elongation in treated compared to control eyes. CID for the FD-only group is significantly larger than that of both FD + HyA and FD + Sham groups (Kruskal-Wallis test, $P < 0.05$). (**B**) Changes in axial lengths of treated (*black boxes*) and control (*gray boxes*) eyes. Change in axial length was significantly larger in treated compared to control eyes in the FD-only group, but not in the FD + HyA or FD + Sham group (Wilcoxon test, $P < 0.05$).

Investigative Ophthalmology & Visual Science

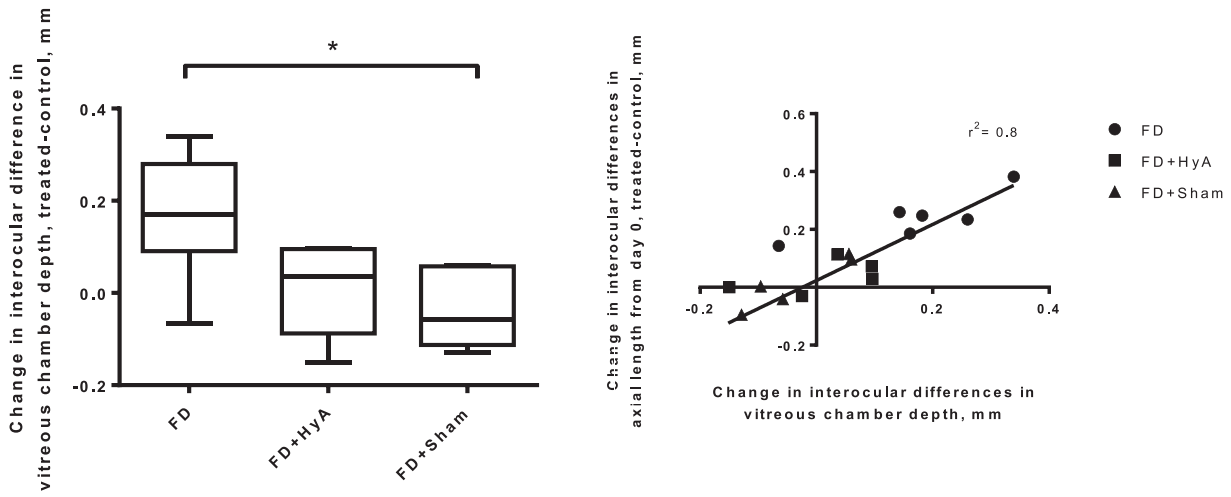

Figure 5. (**A**) Box and whisker plots of change in interocular difference in vitreous chamber depth for FD-only, FD + HyA, and FD + Sham groups over the 28-day study period. *Box* encompasses upper and lower data quartiles; *whiskers* illustrate the upper and lower extremes of the data. Positive values indicate greater elongation in treated compared to control eyes. Differences between the FD-only and FD + Sham groups were significant ($P < 0.05$, Kruskal-Wallis test). (**B**) CID in axial length plotted against CID in vitreous chamber depth for the 28-day study period and FD-only, FD + HyA, and FD + Sham groups (correlation significant, $P < 0.001$).

control eyes of either FD + HyA or FD + Sham groups (1.00 ± 0.05 vs. 1.01 ± 0.05 cyc/deg and 0.99 ± 0.09 vs. 0.96 ± 0.04 cyc/deg, respectively, mean ± SD, Wilcoxon test). Not surprisingly, there was also no significant difference between the groups (interocular differences in visual acuities −0.01 ± 0.08 and 0.02 ± 0.06 cyc/deg for FD + HyA and FD + Sham, respectively, $P = 0.28$, mean ± SD, Mann-Whitney U test). There were also no significant differences in IOPs between the treated and control eyes of the FD + HyA or FD + Sham groups (18.47 ± 10.84 vs. 17.81 ± 9.26 mm Hg for the FD + HyA group, $P = 0.62$; 19.79 ± 6.41 vs. 19.07 ± 6.72 mm Hg for the FD + Sham group, $P = 0.44$, Wilcoxon test). Interocular differences in IOPs for these two groups were also not significantly different from each other (0.66 ± 2.26 mm Hg for FD + HyA group versus 0.73 ± 1.75 mm Hg for FD + Sham group; $P = 0.89$, Mann-Whitney U test).

Histology

At the end of the study, eyes were processed for histology to evaluate the effects of the surgeries on ocular morphology. Sample sections are shown in Figure 8. In eyes treated with hydrogel, remnants of the implant were still clearly visible between the sclera and Tenon's capsule. Extensive cell infiltration was observed in the implant, as evidenced by the numerous stained cell nuclei visible within the hydrogel (see arrows). Interestingly, the adjacent Tenon's capsule in the hydrogel-treated eyes appeared thickened. Similar thickening of Tenon's capsule was also evident in eyes receiving the sham injection. In both cases the capsules also appeared structurally more disorganized than normal.

Additional histologic sections from an eye from the FD + Sham group (Figs. 9A, 9B) revealed the presence of scar-like

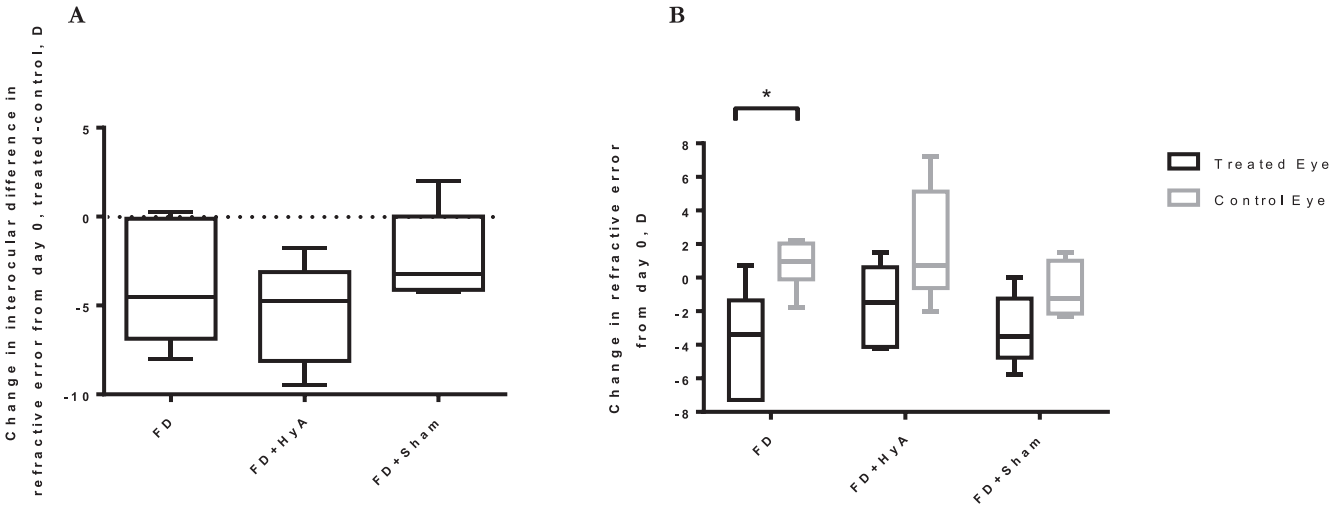

Figure 6. Box and whisker plots of (**A**) change in interocular difference in refractive error and (**B**) change in refractive error for treated and control eyes of FD-only, FD + HyA, and FD + Sham groups over the 28-day study period. *Box* encompasses upper and lower data quartiles; *whiskers* illustrate the upper and lower extremes of the data. (**A**) Changes in refractive error (treated minus control) for all three treatment groups; CIDs were not statistically significant (Kruskal-Wallis test). (**B**) Changes in refractive error of treated (*black bars*) and control (*gray bars*) eyes. Change in refractive error was significantly different in the FD-only group, but not in the FD + HyA or FD + Sham group (Wilcoxon test, $P < 0.05$).

Investigative Ophthalmology & Visual Science

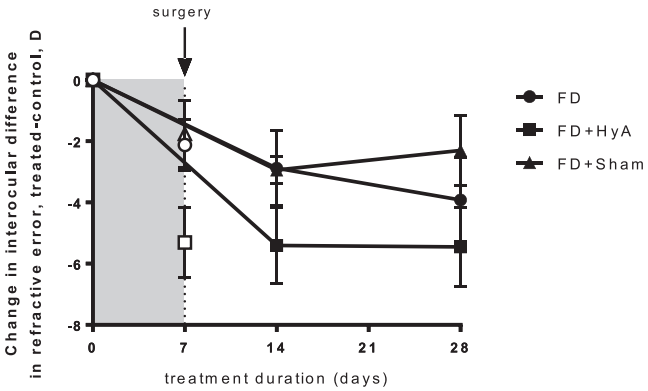

Figure 7. Changes in interocular differences for refractive errors (mean ± SEM) over time for all three groups, all measured under cycloplegia with the exception of the day of surgery (day 7, *open symbols*) when cycloplegia was avoided. *Shaded area* demarcates presurgery treatment period.

tissue confined to the region manipulated in the surgery; no such changes were apparent in regions not disturbed during the surgery (Figs. 9C, 9D).

Discussion

This paper presents the results of the in vivo trial of an injectable HyA hydrogel intended as a scleral-based therapy for control of myopia progression. Prior to this study, the biocompatibility of the HyA hydrogel had been demonstrated for primary guinea pig scleral fibroblasts through in vitro proliferation and migration assays.[55,62] The hydrogel (or buffer in the control group) was injected under Tenon's capsule at the posterior pole of guinea pig eyes, which were first subjected to a short period of FD to induce myopia. To be included in the surgical phase of the study, FD eyes had to have elongated by at least 50 μm more than their contralateral controls. This imposed condition is consistent with the study goal, which was to test the efficacy of an implantable hydrogel in inhibiting the excessive ocular elongation that underlies myopia. For the same reason, FD was chosen over negative lenses to induce myopia since it imposes an open-loop condition and ensured that the stimulus to increased ocular growth was maintained while the treatment was in place.[42] The hypothesis underlying this therapy is that a degradable scaffold compatible with cell infiltration and proliferation, implanted adjacent to the sclera, would allow scleral fibroblasts to migrate into the hydrogel and deposit new matrix that would serve to thicken and strengthen the native sclera. In this way, the implant should afford a degree of protection against excessive ocular elongation and, in the case of existing significant myopia, against continued scleral creep and subsequent myopia progression. Results revealed that the hydrogel itself may not be necessary to control myopia progression in the short term, as both the hydrogel- and buffer-treated groups exhibited slowed eye growth. However, the fact that the implanted hydrogel provides a platform for infiltration of scleral cells and deposition of additional ECM cannot be ignored. Further long-term studies are necessary to determine how enduring the myopia-control effects of these treatments are.

Postmortem histologic analyses revealed that the implants were present 3 weeks after the implantation surgery. This is an important observation, as the hydrogel's effect on ocular growth is likely to be short-lived if it is too rapidly degraded. The results of histologic analysis of the implant and adjacent tissues (sclera and Tenon's capsule) also confirmed the biocompatibility of the hydrogel, as evidenced by extensive cell infiltration, providing further validation of our choice of an HyA-based hydrogel for our myopia-control studies. Interestingly, the nuclei of the cells in the implanted hydrogel were more rounded than the nuclei of fibroblasts in the native sclera. This suggests that despite the hydrogel's ability to support cell migration, it lacked some critical feature of the native sclera required for the retention of the scleral fibroblasts' normal phenotype. We also observed this phenomenon in in vitro migration studies, in which primary guinea pig scleral fibroblasts were allowed to migrate from a glass coverslip into the HyA hydrogel.[55,62] Differences in biophysical characteristics between the hydrogel and sclera may be a

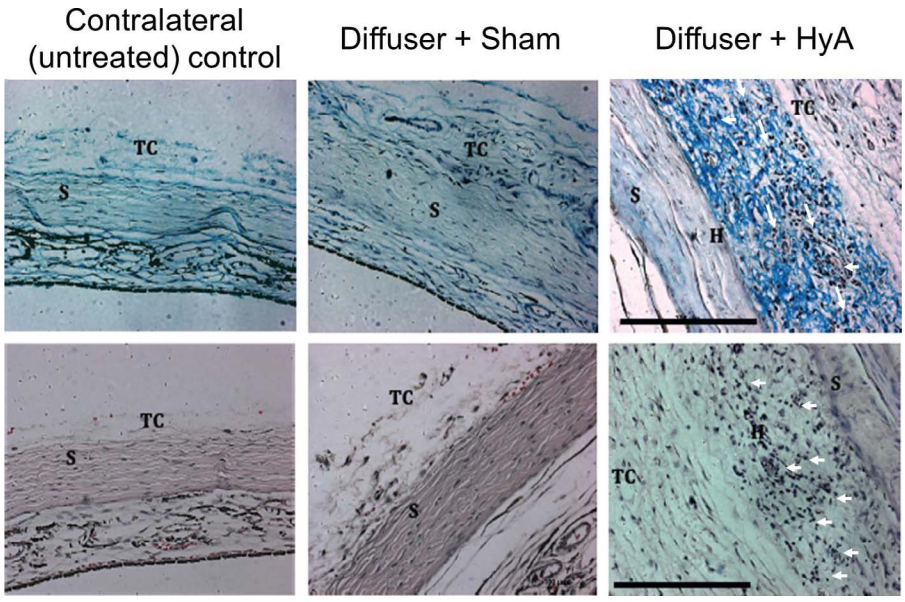

Figure 8. Guinea pig eyes stained with hematoxylin and alcian blue (*top row*) or hematoxylin and eosin (*bottom row*). *Scale bars* represent 200 μm. *Arrows* indicate the nuclei of some of the many cells within the hydrogel. S, sclera, TC, Tenon's capsule, H, hydrogel. Note the thicker Tenon's capsules in the FD + HyA and FD + Sham eyes.

Investigative Ophthalmology & Visual Science

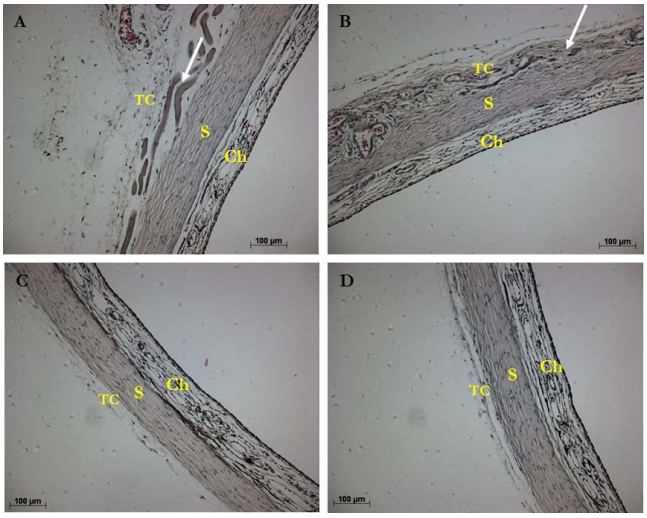

Figure 9. Section of FD + Sham eyes stained with hematoxylin and eosin. (**A**, **B**) Surgical site highlighted, with the *arrow* in (**A**) indicating possible presence of blood and the *arrow* in (**B**) highlighting thickened scar-like tissue. (**C**, **D**) The posterior hemisphere of the same eye shown in (**A**, **B**). This area was inferior to the optic nerve and was not penetrated by the blunt sub-Tenon's needle. Note that the Tenon's capsule appeared tightly fixed to the sclera in (**C**, **D**), suggesting that the buffer injection did not permanently separate these two layers. S, sclera; Ch, choroid; TC, Tenon's capsule.

contributing factor to such differences in cell morphology. In the native sclera, cells are enclosed in a dense collagen scaffold, leaving them little room to "round up." Furthermore, there are likely differences in the biomechanical forces experienced in each of these environments, which may also have contributed to the differences in cell shape. For example, the native sclera is substantially stiffer than the hydrogel (2.09 ± 0.99 MPa for guinea pigs).[63] Scleral fibroblasts in their native environment also experience constant stress, resulting from IOP and tension from attached extraocular muscles.[64] As these stresses would not transfer to the recently implanted and only loosely attached hydrogel, cells migrating into the hydrogel would be free to adopt more rounded shapes. The potential importance of such environmental influences has been demonstrated in in vitro studies of isolated human and chick scleral fibroblasts, which have reported differential expressions of MMPs and matrix components after being exposed to strain.[54,65,66] In another study, isolated cultured pig scleral cells were found to behave differently from those in cultured pieces of sclera, and exposing such tissue to simulated IOP fluctuations introduced further behavioral differences.[67,68] Assuming that the migrating cells ultimately break down the hydrogel and synthesize their own collagen-based ECM, one might expect them to also adopt a more classical scleral phenotype over time. Protein arrays on the recovered hydrogels (i.e., removed at timed intervals after implantation) could be used to test both the latter assumption and the general effect of the hydrogel on cell behavior.[39] Likewise, immunohistochemical studies on recovered hydrogels would address the unresolved question of to what extent inflammatory cells contribute to the cells resident in the hydrogel.

Despite the apparent lack of scleral thickening as determined by A-scan ultrasonography, histologic images revealed thickening of the overlying Tenon's capsule in the areas manipulated during the surgery. These areas also appeared less organized. Thickening of Tenon's capsule may reflect an inflammatory response to the trauma of the surgery, which involved mechanical separation of Tenon's capsule from the underlying sclera. Assuming that these changes translate into increased mechanical stabilization of the posterior sclera, one could predict slowed eye growth, as observed. Specifically, at the end of the 28-day study period, the total elongation of the treated eyes in the FD + HyA group was nearly identical to that of their fellow untreated controls despite the continued presence of the diffusers as a myopia-inducing stimulus. However, these changes were not sufficient to prevent eyes from growing altogether, a finding relevant to safety and potential application as a therapy for the still-growing eyes of children.

The thickening of Tenon's capsule in the FD + Sham group, similar to that seen in the FD + HyA group, was an unexpected finding but offers a potential explanation for some of the myopia-control effects observed with the sham surgery—that the thickened Tenon's capsule increased the mechanical stability of the posterior scleral wall. We interpret this effect on Tenon's capsule (and eye growth) as a wound-healing response, given that the initial surgical incision through the conjunctiva and Tenon's capsule unavoidably results in some disruption of these tissues and of local vascular networks.[69] Even a mild inflammatory/wound-healing reaction may be sufficient to alter the mechanical properties of the posterior Tenon's capsule–sclera complex, if the affected area is sufficiently large. Consistent with this hypothesis, histologic sections from an eye subjected to the FD + Sham treatment (Figs. 9A, 9B) revealed the presence of scar-like tissue confined to the region directly affected by the surgery; no such changes are apparent in regions not manipulated during the surgery (Figs. 9C, 9D).

While we cannot rule out the possibility that our hydrogel implants themselves had an inhibitory effect on axial elongation, the similarity of results for the FD + HyA and FD + Sham groups points to influences on axial elongation related to the surgical procedure itself. The design of our study also does not allow us to distinguish between the effects of the surgery and the injected TEA buffer, although any effect of the latter is likely to be short-lived due its rapid escape from the injection site. Nonetheless, it is possible that both act in concert to trigger a wound-healing response and subsequent thickening of Tenon's capsule, at least initially.

Results showing strong ocular growth inhibition after the surgery logically lead to questions about retinal health, and whether the surgery (injected hydrogel and/or buffer) caused damage to the retina, perhaps contributing to the observed ocular growth inhibition. Flash ERGs are a commonly used tool for assessing retinal function. Of the components making up the ERG waveform, the b-wave is reported to be attenuated in eyes with disrupted retinal blood flow in humans[70] and animals (rabbits),[71] and both a- and b-waves have been shown to be affected by impaired choroidal blood flow.[72,73] Thus any damage to critical ocular vasculature, either incurred during the surgery or resulting from mechanical compression by the implant, might be expected to affect a- and/or b-wave components. While recordings from treated eyes exhibited, on average, slightly lower wave amplitudes and longer implicit times than those from their fellow controls, none of these differences were statistically significant. Importantly, the lack of differences in a- and b-wave amplitudes and implicit times between treated and control eyes suggest that neither surgery (with buffer or hydrogel) adversely affected retinal health.

Visual acuities provide further information about retinal function, mostly at the level of the inner retina. We found no significant differences in the acuities of treated and control eyes for any of the three groups, which were also not different in terms of their interocular differences. These visual acuity findings are consistent with our ERG results, from which we

conclude that neither surgery adversely affected the retina (due to toxicity or mechanical trauma).

An additional perspective on the safety of the therapy is provided by IOP data. It was possible that the space-occupying HyA implants would elevate IOPs. However, we found no evidence of such effects. Specifically, for the FD + HyA as well as the FD + Sham group, no differences between the treated and control eyes were observed. Furthermore, measured IOPs were similar to those recorded with the same tonometer in an independent study of untreated (nonmyopic) guinea pigs conducted in our laboratory.[74]

In addition to the myopia-control outcomes previously discussed, the results from ERG, visual acuity, and IOP measurements support the application of this HyA-based hydrogel as a tool for ocular therapy. These safety studies open doors for its future use as a vehicle for sustained drug and/or cell delivery. Specifically, as a tool for the sustained delivery of drugs to treat posterior segment diseases, it has much to recommend it over repeated, more frequent injections. Moreover, the hydrogel's modularity and adaptability make it an ideal vehicle for the delivery of cells, with potential application in the treatment of neurodegenerative diseases,[75,76] limbal stem cell deficiency,[77] and corneal epithelial defects.[78] In the context of myopia it is also plausible that the application of this hydrogel could be expanded, either to deliver anti-myopia drugs or, in the case of highly myopic eyes with compromised scleras, to deliver replacement cells.

In conclusion, both a posterior sub-Tenon's capsule injection of HyA-based hydrogel and a posterior sub-Tenon's capsule injection of TEA buffer were shown to be safe procedures that can control myopia progression without causing adverse effects on retinal health and IOP. Extensive cell infiltration into hydrogel implants was observed, as was thickening of Tenon's capsule at the surgical site with both surgeries. This work raises the possibility of new and relatively noninvasive surgical approaches to control myopia progression and as a potential substitute for scleral buckling for high myopia. Further studies are warranted to better understand underlying mechanisms and the variables influencing the magnitude and duration of such myopia-control effects.

Acknowledgments

The authors thank John Phillips and his team at the University of Auckland for providing starter animals for our guinea pig colony. They also thank David Hammond and Peter Chen for their assistance measuring refractive errors.

Supported by National Institutes of Health Grants EY019628 (CFW, KEH) and EY012392 (CFW). MBG was funded by a National Science Foundation Graduate Research Fellowship, Ezell Fellowship, and Minnie Turner Award.

Disclosure: **M.B. Garcia**, None; **A.K. Jha**, P; **K.E. Healy**, P; **C.F. Wildsoet**, None

References

1. Curtin B. *The Myopias: Basic Science and Clinical Management*. Philadelphia: Harper & Row; 1985.
2. Holden B, Sankaridurg P, Smith E, Aller T, Jong M, He M. Myopia, an underrated global challenge to vision: where the current data takes us on myopia control. *Eye*. 2014;28:142–146.
3. Jung S, Lee J, Kakizaki H, Jee D. Prevalence of myopia and its association with body stature and educational level in 19-year-old male conscripts in Seoul, South Korea. *Invest Ophthalmol Vis Sci*. 2012;53:5579–5583.
4. Lin L, Shih Y, Hsiao C, Chen C. Prevalence of myopia in Taiwanese schoolchildren: 1983 to 2000. *Ann Acad Med Singapore*. 2004;33:27–33.
5. Vitale S, Sperduto R, Ferris F. Increased prevalence of myopia in the United States between 1971-1972 and 1999-2004. *Arch Ophthalmol*. 2009;127:1632–1639.
6. Hrynchak P, Mittelstaedt A, Machan C, Bunn C, Irving E. Increase in myopia prevalence in clinic-based populations across a century. *Optom Vis Sci*. 2013;90:1331–1341.
7. Williams K, Hammond C. Prevalence of myopia and association with education in Europe. *Lancet*. 2014;383:S109.
8. Lee J-J, Fang P-C, Yang I-H, et al. Prevention of myopia progression with 0.05% atropine solution. *J Ocul Pharmacol Ther*. 2006;22:41–46.
9. Flitcroft D. The complex interactions of retinal, optical and environmental factors in myopia aetiology. *Prog Retin Eye Res*. 2012;31:622–660.
10. Guggenheim J, McBrien N. Form-deprivation myopia induces activation of scleral matrix metalloproteinase-2 in tree shrew. *Invest Ophthalmol Vis Sci*. 1996;37:1380–1395.
11. Rada J, Shelton S, Norton T. The sclera and myopia. *Exp Eye Res*. 2006;82:185–200.
12. Frost M, Norton T. Alterations in protein expression in tree shrew sclera during development of lens-induced myopia and recovery. *Invest Ophthalmol Vis Sci*. 2012;53:322–336.
13. McBrien N, Jobling A, Gentle A. Biomechanics of the sclera in myopia: extracellular and cellular factors. *Optom Vis Sci*. 2009;86:23–30.
14. Moring A, Baker J, Norton T. Modulation of glycosaminoglycan levels in tree shrew sclera during lens-induced myopia development and recovery. *Invest Ophthalmol Vis Sci*. 2007;48:2947–2956.
15. Rada J, Nickla D, Troilo D. Decreased proteoglycan synthesis associated with form deprivation myopia in mature primate eyes. *Invest Ophthalmol Vis Sci*. 2000;41:2050–2058.
16. McBrien N, Gentle A. Role of the sclera in the development and pathological complications of myopia. *Prog Retin Eye Res*. 2003;22:307–338.
17. Siegwart J, Norton T. Regulation of the mechanical properties of tree shrew sclera by the visual environment. *Vision Res*. 1999;39:387–407.
18. Phillips J, Khalaj M, McBrien N. Induced myopia associated with increased scleral creep in chick and tree shrew eyes. *Invest Ophthalmol Vis Sci*. 2000;41:2028–2034.
19. Avetisov E, Savitskaya N, Vinetskaya M, Iomdina E. A study of biochemical and biomechanical qualities of normal and myopic sclera in humans of different age groups. *Metab Pediatr Syst Ophthalmol*. 1984;7:183–188.
20. McBrien N, Cornell L, Gentle A. Structural and ultrastructural changes to the sclera in a mammalian model of high myopia. *Invest Ophthalmol Vis Sci*. 2001;42:2179–2187.
21. Chang L, Pan C, Ohno-Matsui K, et al. Myopia-related fundus changes in Singapore adults with high myopia. *Am J Ophthalmol*. 2013;155:991–999.
22. Grosvenor T. Why is there an epidemic of myopia? *Clin Exp Optom*. 2003;86:273–275.
23. Saw S, Gazzard G, Shih-Yen E, Chua W. Myopia and associated pathological complications. *Ophthalmic Physiol Opt*. 2005;25:381–391.
24. Wollensak G, Spoerl E. Collagen crosslinking of human and porcine sclera. *J Cataract Refract Surg*. 2004;30:689–695.
25. Wollensak G, Iomdina E. Crosslinking of scleral collagen in the rabbit using glyceraldehyde. *J Cataract Refract Surg*. 2008;34:651–656.
26. Liu T, Wang Z. Collagen crosslinking of porcine sclera using genipin. *Acta Ophthalmol*. 2013;91:e253–e257.

27. Liu T-X, Luo X, Gu Y-W, Yang B, Wang Z. Correlation of discoloration and biomechanical properties in porcine sclera induced by genipin. *Int J Ophthalmol*. 2014;7:621–625.
28. Wang M, Corpuz CCC. Effects of scleral cross-linking using genipin on the process of form-deprivation myopia in the guinea pig: a randomized controlled experimental study. *BMC Ophthalmol*. 2015;15:89.
29. Wollensak G, Iomdina E, Dittert D, Salamatina O, Stoltenburg G. Cross-linking of scleral collagen in the rabbit using riboflavin and UVA. *Acta Ophthalmol Scand*. 2005;83:477–482.
30. Il, Ahn J Kuffova L, Merrett K, et al. Crosslinked collagen hydrogels as corneal implants: effects of sterically bulky vs. non-bulky carbodiimides as crosslinkers. *Acta Biomater*. 2013;9:7796–7805.
31. Fagerholm P, Lagali NS, Ong JA, et al. Stable corneal regeneration four years after implantation of a cell-free recombinant human collagen scaffold. *Biomaterials*. 2014; 35:2420–2427.
32. Li W, Long Y, Liu Y, et al. Fabrication and characterization of chitosan-collagen crosslinked membranes for corneal tissue engineering. *J Biomater Sci Polym Ed*. 2014;25:1962–1972.
33. Kishore V, Alapan Y, Iyer R, Mclay R. Applications of hydrogels in ocular tissue engineering. In: Demirci U, Khademhosseini A, eds. In: *GELS Handbook: Fundamentals, Properties, Applications. Volume 2: Applications of Hydrogels in Regenerative Medicine*. Singapore: World Scientific; 2016: 137–164.
34. Avetisov E, Tarutta E, Iomdina E, Vinetskaya M, Andreyeva L. Nonsurgical and surgical methods of sclera reinforcement in progressive myopia. *Acta Ophthalmol Scand*. 1997;75:618–623.
35. Su J, Iomdina E, Tarutta E, Ward B, Song J, Wildsoet C. Effects of poly(2-hydroxyethyl methacrylate) and poly(vinyl-pyrrolidone) hydrogel implants on myopic and normal chick sclera. *Exp Eye Res*. 2009;88:445–457.
36. Su J, Wall S, Healy K, Wildsoet C. Scleral reinforcement through host tissue integration with biomimetic enzymatically degradable semi-interpenetrating polymer network. *Tissue Eng Part A*. 2010;16:905–916.
37. Curtin B, Whitmore W. Long-term results of scleral reinforcement surgery. *Am J Ophthalmol*. 1987;103:544–548.
38. Ward B, Tarutta E, Mayer M. The efficacy and safety of posterior pole buckles in the control of progressive high myopia. *Eye*. 2009;23:2169–2174.
39. Jha A, Tharp K, Ye J, et al. Growth factor sequestering and presenting hydrogels promote survival and engraftment of transplanted stem cells. *Biomaterials*. 2015;47:1–12.
40. Howlett M, McFadden S. Emmetropization and schematic eye models in developing pigmented guinea pigs. *Vision Res*. 2007;47:1178–1190.
41. Zhou X, Qu J, Xie R, et al. Normal development of refractive state and ocular dimensions in guinea pigs. *Vision Res*. 2006; 46:2815–2823.
42. Howlett M, McFadden S. Form-deprivation myopia in the guinea pig (Cavia porcellus). *Vision Res*. 2006;46:267–283.
43. Howlett M, McFadden S. Spectacle lens compensation in the pigmented guinea pig. *Vision Res*. 2009;49:219–227.
44. Jha A, Tharp K, Ye J, et al. Engineered hyaluronic acid-based hydrogels for survival and transplantation of stem cells. Society for Biomaterials; 2014: Abstract 291. Available at: http://abstracts.biomaterials.org/data/papers/2014/0332-000845.pdf. Accessed March 2, 2017.
45. Jha AK, Dashti D, Ye J, Yeghiazarians Y, Healy KE. Hyaluronic acid-based hydrogel for cardiovascular tissue engineering. In: *9th World Biomaterials Congress*. Chengdu, China; 2012.
46. Tharp K, Jha A, Kraiczy J, et al. Matrix-assisted transplantation of functional beige adipose tissue. *Diabetes*. 2015;11:3713–3724.
47. Young T, Scavello G, Paluru P, Choi J, Rappaport E, Rada J. Microarray analysis of gene expression in human donor sclera. *Mol Vis*. 2004;10:163–176.
48. Metlapally R, Jobling A, Gentle A, McBrien N. Characterization of the integrin receptor subunit profile in the mammalian sclera. *Mol Vis*. 2006;12:725–734.
49. Rezania A, Healy K. Biomimetic peptide surfaces that regulate adhesion, spreading, cytoskeletal organization, and mineralization of the matrix deposited by osteoblast-like cells. *Biotechnol Prog*. 1999;15:19–32.
50. Barber T, Harbers G, Park S, Gilbert M, Healy K. Ligand density characterization of peptide-modified biomaterials. *Biomaterials*. 2005;26:6897–6905.
51. Stile R, Healy K. Thermo-responsive peptide-modified hydrogels for tissue regeneration. *Biomacromolecules*. 2001;2: 185–194.
52. Wall S, Yeh C, Tu R, Mann M, Healy K. Biomimetic matrices for myocardial stabilization and stem cell transplantation. *J Biomed Mater Res A*. 2010;95:1055–1066.
53. Siegwart J, Norton T. Selective regulation of MMP and TIMP mRNA levels in tree shrew sclera during minus lens compensation and recovery. *Invest Ophthalmol Vis Sci*. 2005;46:3484–3492.
54. Shelton L, Rada J. Effects of cyclic mechanical stretch on extracellular matrix synthesis by human scleral fibroblasts. *Exp Eye Res*. 2007;84:314–322.
55. Garcia M. *Myopia Control in Guinea Pigs* [doctoral dissertation]. Berkeley, CA: University of California-Berkeley; 2014.
56. Jha A, Hule R, Jiao T, et al. Structural analysis and mechanical characterization of hyaluronic acid-based doubly cross-linked networks. *Macromolecules*. 2009;42:537–546.
57. Gurski L, Jha A, Zhang C, Jia X, Farach-Carson M. Hyaluronic acid-based hydrogels as 3D matrices for in vitro evaluation of chemotherapeutic drugs using poorly adherent prostate cancer cells. *Biomaterials*. 2009;30:6076–6085.
58. Chung EH, Gilbert M, Virdi AS, Sena K, Sumner DR, Healy KE. Biomimetic artificial ECMs stimulate bone regeneration. *J Biomed Mater Res A*. 2006;79:815–826.
59. Schmid GF, Papastergiou GI, Nickla DL, et al. Validation of laser Doppler interferometric measurements in vivo of axial eye length and thickness of fundus layers in chicks. *Curr Eye Res*. 1996;15:691–696.
60. Nickla D, Wildsoet C, Wallman J. Compensation for spectacle lenses involves changes in proteoglycan synthesis in both the sclera and choroid. *Curr Eye Res*. 1997;16:320–326.
61. Nickla D, Wildsoet C, Wallman J. The circadian rhythm in intraocular pressure and its relation to diurnal ocular growth changes in chicks. *Exp Eye Res*. 1998;66:183–193.
62. Garcia M, Morgan A, Jha AK, Healy KE, Wildsoet CF. An in vitro assay to quantify 3D cell migration from intact monolayers into hydrogels. International Myopia Conference; Asilomar, CA; 2013.
63. Wang X, Chen W, Li Y, Gao T. Biomechanical properties of experimental myopia in the guinea pig. In: *The 2nd International Conference on Bioinformatics and Biomedical Engineering (ICBBE 2008)*. Shanghai, China: IEEE Computer Society; 2008:1825–1827.
64. Greene P. Mechanical considerations in myopia: relative effects of accomodation, convergence, intraocular pressure, and extraocular muscles. *Am J Optom Physiol Opt*. 1980;57: 902–914.
65. Cui W, Bryant M, Sweet P, McDonnel P. Changes in gene expression in response to mechanical strain in human scleral fibroblasts. *Exp Eye Res*. 2004;78:275–284.

Investigative Ophthalmology & Visual Science

66. Fujikura H, Seko Y, Tokoro T, Mochizuki M, Shumokawa H. Involvement of mechanical stretch in the gelatinolytic activity of the fibrous sclera of chicks, in vitro. *Jpn J Ophthalmol*. 2002;46:24–30.
67. Ganesan P, Wildsoet C. Design and validation of a bioreactor for scleral tissue. Society for Biomaterials; 2010: Abstract 338. Available at: http://abstracts.biomaterials.org/data/papers/2010/338.pdf. Accessed March 2, 2017.
68. O'Brien PG. *Scleral Bioreactor: Design and Use for Evaluation of Myopia Therapies*. Berkeley, CA: University of California-Berkeley; 2011. Doctoral dissertation.
69. Khaw P, Occleston N, Schultz G, Grierson I, Sherwood M, Larkin G. Activation and suppression of fibroblast function. *Eye (Lond)*. 1994;8:188–195.
70. Nilsson S. Human retinal vascular obstructions. A quantitative correlation of angiographic and electroretinographic findings. *Acta Ophthalmol*. 1971;49:111–133.
71. Noell W. The origin of the electroretinogram. *Am J Ophthalmol*. 1954;38:78–90.
72. Fujino T, Hamasaki D. The effect of occluding the retinal and choroidal circulations on the electroretinogram of monkeys. *J Physiol*. 1965;180:837–845.
73. McLeod D, Hayreh S. Occlusion of posterior ciliary artery. IV. Electroretinographic studies. *Br J Ophthalmol*. 1972;56:765–769.
74. Ostrin LA, Wildsoet CF. Optic nerve head and intraocular pressure in the guinea pig eye. *Exp Eye Res*. 2016;146:7–16.
75. Sieving P, Caruso R, Tao W, et al. Ciliary neurotrophic factor (CNTF) for human retinal degeneration: phase I trial of CNTF delivered by encapsulated cell intraocular implants. *Proc Natl Acad Sci U S A*. 2006;103:3896–3901.
76. Kundu J, Michaelson A, Baranov P, Young M, Carrier R. Approaches to cell delivery: substrates and scaffolds for cell therapy. *Dev Ophthalmol*. 2014;53:143–154.
77. Wright B, Mi S, Connon C. Towards the use of hydrogels in the treatment of limbal stem cell deficiency. *Drug Discov Today*. 2013;18:79–86.
78. Koizumi N, Inatomi T, Suzuki T. Cultivated corneal epithelial stem cell transplantation in ocular surface disorders. *Ophthalmology*. 2001;108:1569–1574.

Investigative Ophthalmology & Visual Science